Vortex-state complex Hall conductivity of superconducting $YBa_2Cu_3O_{7-\delta}$ epitaxial films at radio frequencies

D. A. Beam*†, N.-C. Yeh*††, and R. P. Vasquez**

* Department of Physics, California Institute of Technology, Pasadena, CA 91125.

** Center for Space Microelectronics Technology, Jet Propulsion Laboratory, California Institute of Techonology, Pasadena, CA 91109.

The vortex-state complex Hall conductivity (σ_{xy}) of superconducting $YBa_2Cu_3O_7$ epitaxial films is investigated from DC to radio frequencies (up to 7×10^6 Hz), using a direct transport measurement technique. The experimental results are analyzed in terms of a model generalized from that for the dc Hall conductivity. This generalized model assumes that 1) the occurrence of sign reversal in the dc vortex-state Hall conductivity is the result of different carrier densities within and far away from the vortex core; 2) the Drude approximation is applicable; and 3) the anomalous sign reversal occurs in the flux-flow limit. We find that the temperature and frequency dependencies of our complex Hall conductivity data are in good agreement with our phenomenological model. In addition, when extended to higher frequencies, the same model provides consistent description for the complex Hall conductivity data at 100 – 800 GHz. Moreover, the magnetic field (B) dependence of the complex Hall conductivity data reveals that both vortices (σ_{xy}^v) and quasiparticles (σ_{xy}^q) contribute to the vortex state Hall conduction, where $\sigma_{xy}^v \propto B^{-1}$ and $\sigma_{xy}^q \propto B$, in agreement with the model. The magnitude of the real part, σ_{xy}', is also consistent with the theoretical estimate, while the magnitude of the imaginary part, σ_{xy}'', is significantly larger than the theoretical prediction. This discrepancy may be attributed to the unconventional electronic structures in vortices of cuprate superconductors with d-wave or mixed pairing symmetries.

PACS: 74.60.Ge, 74.60.Ec, 74.25.Dw, 74.72.Bk

---

† Current address: Sikorsky Aircraft Corporation, Stratford, CT 06615.

†† Corresponding author. E-mail address: ncyeh@caltech.edu

I. Introduction

The anomalous sign reversal in the vortex-state Hall conductivity (σ_{xy}) of extreme type-II superconductors is an outstanding issue that has attracted much attention [1-14]. Although quantitative description for the microscopics of the vortex-state Hall conduction remains incomplete, several important facts have been established. First, the sign reversal is associated with intrinsic physical properties of type-II superconductors [2,3,10-15], and is independent of either random [4] or correlated disorder [8,12]. Second, the occurrence of sign reversal in σ_{xy} has been attributed to the non-uniform spatial distribution of carriers within and far outside the vortex core [10-12]. Third, the dc vortex-state Hall conductivity of superconducting cuprates is found to be strongly dependent on the doping level, showing anomalous sign reversal in the underdoped regime and no anomaly in the overdoped regime [13]. This important experimental finding suggests the relevance of the electronic structures within vortices to the Hall conductivity in the superconducting state, although the dependence of the sign of σ_{xy} [13] is opposite to the prediction based on the s-wave weak coupling theory [10,11,14,15]. Recent theoretical investigation of the electronic structure of vortices in high-temperature superconducting cuprates (HTSC) has revealed novel properties associated with the d-wave pairing symmetry [16], which may lead to better understanding of the doping-level dependence. Fourth, the characteristic time associated with the vortex-state Hall conductivity of high-temperature superconductors has been estimated from both dc [12] and microwave [17] measurements, and is found to be comparable to the quasiparticle life time.

Despite increasing knowledge for the vortex-state Hall conductivity, most experimental results and the corresponding theoretical interpretation have only focused on the dc Hall effect, except the coherent time-domain spectroscopy measurements [7] of the complex Hall conductivity on a $YBa_2Cu_3O_{7-\delta}$ epitaxial film at 100 $\sim$ 800 GHz. The frequency and temperature dependence of the high-frequency Hall conductivity was analyzed in terms of a simple two-fluid model, and the vortex-state Hall conductivity was entirely attributed to the contribution of quasiparticles. The latter conclusion contradicts experimental results

obtained in the dc limit, where the vortex-state Hall conductivity is known to consist of contributions from both vortices and quasiparticles [2,5,9,12]. It is therefore important to reconcile the difference between the high-frequency and dc measurements by investigating the complex Hall conductivity at intermediate frequencies.

In this work, we report experimental studies of the complex vortex-state Hall conductivity of $YBa_2Cu_3O_{7-\delta}$ epitaxial thin films at frequencies from 10^2 to 10^7 Hz. Our experimental results indicate that in the anomalous sign-reversal regime of $\sigma_{xy}(= \sigma'_{xy} - i\sigma''_{xy})$, where σ'_{xy} is the real part and σ''_{xy} is the imaginary part, the frequency dependence of the complex Hall conductivity follows $\sigma'_{xy} \sim$ constant, $\sigma''_{xy} \propto \omega$, where ω is the angular frequency of the applied ac currents. The experimental results are analyzed in terms of a model generalized from that [10] for the dc Hall conductivity. This generalized model is based on the Drude approximation [18] in the flux-flow limit, and it assumes that the occurrence of sign reversal in the dc vortex-state Hall conductivity is the result of different carrier densities within and far away from the vortex core. We find that the temperature and frequency dependencies of our data, as well as the data taken at much higher frequencies (100 – 800 GHz), are in good agreement with this phenomenological model. In addition, the magnetic field (B) dependence of the complex Hall conductivity data is consistent with contributions from both the core states of vortices (σ^v_{xy}) and the quasiparticle contribution (σ^q_{xy}), where $\sigma^v_{xy} \propto B^{-1}$ and $\sigma^q_{xy} \propto B$. Furthermore, $|\sigma''_{xy}| \ll |\sigma'_{xy}|$, and the magnitude of σ'_{xy} is consistent with known physical parameters. On the other hand, we find that the empirical $|\sigma''_{xy}|$ is much larger than the theoretical prediction. Possible origins for this discrepancy, including the unconventional electronic structures in vortices of cuprate superconductors, are discussed.

This paper is structured as follows. In Section II we review the theoretical model for the dc vortex-state Hall conductivity by Feigel'man et al. [10], and generalize the d formalism to complex Hall conductivity under the Drude approximation. Section III a description of the broad-band direct transport measurement techniques for the comple Hall conductivity. In Section IV, the experimental results are presented and compared wit

the predictions of our model. Section V consists of a discussion of the physical significance of our data, and compares our results with related literature. Finally, a summary of the key findings of this work is given in Section VI.

II. Flux-Flow Vortex-State Hall Conductivity in the Drude Approximation

A. dc Hall conductivity

The starting point of our approach is a phenomenological description for the dc vortex-state Hall conductivity by Feigel'man, Geshkenbein, Larkin and Vinokur (FGLV) [10]. The FGLV model assumes two primary contributions to the vortex-state Hall conductivity. One is the vortex Hall conductivity (σ_{xy}^{v}), the other is the quasiparticle contribution (σ_{xy}^{q}). The sign of σ_{xy}^{q} is the same as that of the normal state and is linearly proportional to the magnetic induction B, whereas σ_{xy}^{v} arises from the electron-hole asymmetry [15] and is dependent on details of the density of states [14,15]. It is believed that the vortex contribution σ_{xy}^{v} is responsible for the observed sign reversal in the Hall conductivity of various type-II superconductors. Assuming the BCS Hamiltonian, van Otterlo et al. [11] have shown that σ_{xy}^{v} may be interpretted as the vortex charging effect that arises from the difference in the carrier density within the vortex core and that far outside of the vortex core, and this difference yields a sign change in the vortex-state Hall conductivity relative to that of the normal-state Hall conductivity if $\partial(\ln T_c)/\partial\mu|_{\mu=E_F} < 0$ [13], where μ is the chemical potential and E_F the Fermi energy. Hence, a phenomenological description for the vortex-state Hall conductivity is given by the following expression (in SI units) [10]:

$$\sigma_{xy} = \sigma_{xy}^{v} + \sigma_{xy}^{q} = \left\{ \frac{ne}{B}\left[g\frac{(\omega_0\tau)^2}{1+(\omega_0\tau)^2} - \frac{\delta n}{n}\right]\right\} + (1-g)\left[\frac{ne}{B}\frac{(\omega_c\tau)^2}{1+(\omega_c\tau)^2}\right], \qquad (1)$$

where σ_{xy}^{v} is the vortex contribution consisting of effects of the bound-state quasiparticles within the vortex cores and the vortex charging effect, and σ_{xy}^{q} is the contribution from all other quasiparticles. Here n denotes the total carrier density, $\delta n(\equiv n_0 - n_\infty)$ is the difference between the carrier density within the vortex core (n_0) and that far outside the vortex core

(n_∞), and δn satisfies the conditions $\delta n \ll n(\approx n_0 \approx n_\infty)$, $\delta n \rightarrow$ constant for $T \rightarrow 0$ and $\delta n \rightarrow 0$ for $T \rightarrow T_c^-$; $\hbar\omega_0 = \Delta_0^2/E_F$ is the energy level of the vortex bound state for an s-wave superconductor with a finite energy gap Δ_0 [19]; $\omega_c \equiv (eB/m^*)$ is the cyclotron frequency of normal carriers; g is a function dependent on the ratio of $[\Delta_0/(k_BT)] \equiv x$, which satisfies the conditions $g(x \gg 1) \rightarrow 1$ and $g(x \rightarrow 0) \approx x$ [10]. In the event that $\delta n > 0$, sign reversal in σ_{xy} can take place as the temperature is varied [10,11]. We note that except for the term associated with the non-uniform spatial distribution of the carriers, $(\delta n/n)$, the FGLV model in Eq.(1) is essentially based on the Drude approximation, which assumes one characteristic time τ for both quasiparticles outside the vortex cores and bound-state quasiparticles inside the vortex cores. It is implicitly understood that τ is a strong function of the temperature, and that the temperature dependence of τ in the superconducting state is expected to be different from that in the normal state. We also note that the FGLV formalism is only applicable to isotropic superconductors. However, Eq.(1) can be easily generalized for anisotropic superconductors [12] by performing the anisotropic-to-isotropic scaling transformation [6,20].

When examining the term $[-(ne/B)(\delta n/n)] \equiv \delta\sigma_{xy}$ in Eq.(1) more closely, we remark that this contribution due to the vortex charging effect implicitly assumes a very long relaxation time τ_∞ associated with δn, such that $\omega_c\tau_\infty \gg 1$ for finite magnetic fields in the superconducting state. This assumption implies that the charge imbalance associated with the presence of vortices is long lived relative to all other relevant time scales in the vortex state, so that its contribution to the Hall conductivity is analogous to that of the free electron gas. Hence, we may rewrite $\delta\sigma_{xy}$ in terms of the following approximation:

$$\begin{aligned}
\delta\sigma_{xy} = \frac{(-\delta n)e^2\tau_\infty}{m^*}\frac{\omega_c\tau_\infty}{1+\omega_c^2\tau_\infty^2} &= \left(-\frac{\delta n}{n}\right)\frac{\sigma_0}{\omega_c\tau}\frac{\omega_c^2\tau_\infty^2}{1+\omega_c^2\tau_\infty^2} \\
&\approx \left(-\frac{\delta n}{n}\right)\frac{ne}{B}, \qquad \text{if } \omega_c\tau_\infty \gg 1 \text{ for } T < T_c; \\
&\approx 0, \qquad\qquad\qquad \text{if } B \rightarrow 0 \text{ and } \omega_c\tau_\infty \ll 1,
\end{aligned}$$

where $\sigma_0 \equiv (ne^2\tau/m^*)$ is the normal state dc conductivity in the Drude approximation. The above clarification is useful for us to generalize the FGLV model from dc to finite frequencies, as discussed below.

B. Complex Hall conductivity

Before extending the FGLV formula to finite frequencies in the Drude approximation, we first review the equation of motion for a charge carrier in the normal state for magnetic field ($\vec{B}$) parallel to the $\hat{z}$-axis:

$$\frac{d\vec{p}}{dt} = e\left[\vec{E} + \frac{\vec{p}}{m} \times \vec{B}\right] - \frac{\vec{p}}{\tau} \qquad (2),$$

where $\vec{p} = p_x\hat{x} + p_y\hat{y}$ denotes the momentum of carriers, $\vec{E} = E_x\hat{x} + E_y\hat{y}$ is the electric field, and τ is the tranport relaxation time. Assuming linear response so that $d\vec{p}/dt = -i\omega\vec{p}$, where ω is the angular frequency of the applied ac currents, the normal state complex longitudinal and Hall conductivities may be easily derived from the equation of motion. We find that

$$\begin{aligned} \sigma^n_{xx} &= \frac{(1 - i\omega\tau)\sigma_0}{[1 + (\omega_c^2 - \omega^2)\tau^2] - i2\omega\tau}, \\ \sigma^n_{xy} &= \frac{\omega_c\tau}{(1 - i\omega\tau)}\sigma^n_{xx}, \\ &= \frac{(\omega_c\tau)\sigma_0}{[1 + (\omega_c^2 - \omega^2)\tau^2] - i2\omega\tau}. \end{aligned} \qquad (3)$$

For the superconducting state, we assume the flux-flow limit where the effects of pinning can be neglected. We argue that this assumption is justified in the derivation of the vortex-state Hall conductivity, because it has been verified both experimentally [8,12] and theoretically [4] that pinning effects on vortices do not influence the vortex-state Hall conductivity. Taking the linear response limit and assuming two contributions σ^v_{xy} and σ^q_{xy} as in Eq.(1), and noting that the characteristic frequency ω_0 of the bound-state quasiparticles is associated with an effective magnetic field H_{c2} rather than B, (such that $\omega_0 \equiv \Delta_0^2/(\hbar E_F) \sim eH_{c2}/m^*$), the complex longitudinal and Hall conductivities may be derived from the equation of motion. We obtain:

$$\begin{aligned} \sigma_{xx} &= \sigma^v_{xx} + \sigma^q_{xx}, \\ &= \left\{g\left(\frac{\sigma_0}{\omega_c\tau}\right)\frac{(1 - i\omega\tau)\omega_0\tau}{[1 + (\omega_0^2 - \omega^2)\tau^2] - i2\omega\tau}\right\} + \left\{(1 - g)\frac{(1 - i\omega\tau)\sigma_0}{[1 + (\omega_c^2 - \omega^2)\tau^2] - i2\omega\tau}\right\} \end{aligned} \qquad (4a)$$

$$\sigma_{xy} = \sigma_{xy}^{v} + \sigma_{xy}^{q}, \tag{4b}$$
$$= \frac{ne}{B}\left\{\frac{g(\omega_0^2\tau^2)}{[1+(\omega_0^2-\omega^2)\tau^2]-i2\omega\tau} - \frac{(\delta n/n)(\omega_c^2\tau_\infty^2)}{[1+(\omega_c^2-\omega^2)\tau_\infty^2]-i2\omega\tau_\infty} + \frac{(1-g)\omega_c^2\tau^2}{[1+(\omega_c^2-\omega^2)\tau^2]-i2\omega\tau}\right\}.$$

We note that both σ_{xx} and σ_{xy} have been given for the sake of consistency, although we are primarily interested in the complex Hall conductivity rather than the longitudinal conductivity, and that only σ_{xy} is independent of pinning defects in the superconductor. Furthermore, in Eq.(4a) we have assumed $\sigma_{xx}^{v} \propto g(H_{c2}/B)\sigma_0 \sim g(\omega_0/\omega_c)\sigma_0$, to ensure that the longitudinal conductivity is consistent with the flux-flow conductivity. We also note that in the dc limit ($\omega \to 0$) and for $\omega_c\tau_\infty \gg 1$, σ_{xy} recovers the expression in Eq.(1).

To verify the validity of our approach, it is interesting to compare $\sigma_{xx}(=\sigma_{xx}' - i\sigma_{xx}'')$ in the zero-magnetic field with that in the vortex state. That is, the quantity $g(H_{c2}/B)$ in the flux-flow limit may be replaced by the superfluid fraction (n_s/n) for $B \to 0$, such that in the low temperature and high-frequency limit where $g \to 1$ and $\omega\tau \gg \omega_0\tau \gg 1$, we obtain

$$\sigma_{xx} \approx i\frac{n_s e^2}{m^*\omega} = -i\sigma_{xx}'', \tag{5}$$

consistent with Mattis-Bardeen theory [21]. On the other hand, for $T > T_c$ and $B = 0$, the superfluid fraction vanishes, and Eq.(4a) recovers the Drude conductivity for normal metals, $\sigma_{xx}(\omega) = \sigma_0/(1 - i\omega\tau)$. Recasting σ_{xx} into complex resistivity ρ_{xx} and taking $\rho_0 \equiv (1/\sigma_0)$, we obtain

$$\frac{\rho_{xx}'(\omega)}{\rho_0} = \frac{(\sigma_{xx}'/\sigma_0)}{(\sigma_{xx}'/\sigma_0)^2 + (\sigma_{xx}''/\sigma_0)^2} \approx 0, \qquad (T \ll T_c)$$
$$\approx 1; \qquad (T \gg T_c)$$
$$\frac{\rho_{xx}''(\omega)}{\rho_0} = \frac{-(\sigma_{xx}''/\sigma_0)}{(\sigma_{xx}'/\sigma_0)^2 + (\sigma_{xx}''/\sigma_0)^2} \approx \omega\tau, \qquad \text{(for both } T \ll T_c \text{ and } T \gg T_c). \tag{6}$$

We shall show in the next section that the above approach is indeed in good agreement with our experimental observation at radio frequencies, and in the high-frequency limit is also consistent with the experimental data taken with the coherent time-domain spectroscopy [7].

Next, we consider the complex Hall conductivity σ_{xy} under our experimental condition. Using $m^* = 4m_e$ [13,22] and $\tau \sim 10^{-13}$ s near T_c [12,23,24], we find that $\omega_c\tau \sim 5 \times 10^{-3}B$ for $B(\approx H)$ measured in Tesla, and $\omega\tau \ll \omega_c\tau, \omega_0\tau$ is satisfied for the range of frequency and magnetic field of our experiments. In this limit, the real and imaginary parts of σ_{xy} become:

$$\sigma'_{xy}(\omega) \approx \frac{ne}{B}\left[g\frac{\omega_0^2\tau^2}{1+\omega_0^2\tau^2} - \left(\frac{\delta n}{n}\right)\right] + (1-g)\frac{ne}{B}\left[\frac{\omega_c^2\tau^2}{1+\omega_c^2\tau^2}\right],$$
$$\sigma''_{xy}(\omega) \approx (-2\omega\tau)\frac{ne}{B}\left[g\frac{\omega_0^2\tau^2}{(1+\omega_0^2\tau^2)^2} - \frac{(\delta n/n)}{\omega_c^2\tau\tau_\infty} + (1-g)\frac{\omega_c^2\tau^2}{(1+\omega_c^2\tau^2)^2}\right]. \qquad (7)$$

Therefore σ'_{xy} is nearly frequency independent for all temperatures if $\omega \ll (\omega_c, \omega_0)$, and is consistent with the dc Hall conductivity expression in Eq.(1). On the other hand, in the same frequency range, the relation $|\sigma''_{xy}| \propto \omega$ holds for all temperatures. We shall show later that the frequency dependence of both σ'_{xy} and σ''_{xy} in Eq.(7) is indeed consistent with our experimental results. Furthermore, we shall verify the validity of Eq.(4b) in the high-frequency limit by comparing Eq.(4b) with the data taken with the coherent time domain spectroscopy [7].

III. Experimental

There have been limited direct ac transport measurements of superconductors in the radio frequency (*rf*) range, largely due to difficulties in resolving small impedance of the superconductor from a large background of parasitic impedances and noises that are associated with the electronic instruments and cables. Recently, several direct ac longitudinal impedance measurements of high-temperature superconductors have been reported in the literature [25-29], and these experiments focused on critical scaling analysis of the vortex phase transitions associated with different types of controlled disorder. To the best of our knowledge, there has not been any report of direct transport measurements of the complex Hall conductivity at *rf* frequencies, possibly because the Hall angle in high-temperature superconductors is small, so that the signals of Hall impedance are orders of magnitude

smaller than those of the longitudinal impedance, making the signal of the Hall impedance very difficult to resolve. In this work, we extend our previous ac measurement techniques for the longitudinal conductivity [25-30] to the Hall effect studies [31].

In a superconductor with uniaxial symmetry along the $\hat{z}$-axis, the Hall conductivity for magnetic field parallel to $\hat{z}$ is determined by the longitudinal and Hall resistivities, ρ_{xx} and ρ_{xy}, according to the following formula:

$$\sigma_{xy} = \frac{\rho_{xy}}{\rho_{xx}^2 + \rho_{xy}^2}, \tag{8}$$

where $\rho_{xy}(\vec{H}) = -\rho_{yx}(\vec{H})$ is satisfied through the Onsager relations [32], and $\rho_{xx} = \rho_{yy}$ as measured after the van der Pauw corrections [33]. Hence, both the complex ρ_{xx} and ρ_{xy} must be determined in order to obtain the complex Hall conductivity. In this work, we restrict our measurements to temperatures where both ρ_{xx} and ρ_{xy} are independent of the applied currents, because the van der Pauw corrections are only valid in the linear response limit [33], and because large errors in the low temperature σ_{xy} data are likely to occur due to the rapidly vanishing ρ_{xx} and ρ_{xy} [12]. We describe in the following our experimental approaches for obtaining the complex components of ρ_{xx} and ρ_{xy}. We note that ρ_{xx} and ρ_{xy} respond differently to the reversal of magnetic field, so that different calibration procedures are employed to obtain these components.

To obtain the ac resistivity ρ_{xx}, we use similar experimental set up and calibration procedure developed previously [25-30], with minor modifications in the electronic components [31] to improve the signal-to-noise ratio and to extend the measurement frequency range from previous 100 Hz $\sim$ 2 MHz to 100 Hz $\sim$ 7 MHz. The ac impedance is measured using the four-point technique, and the signal is first amplified with a low-noise, 42 dB-gain pre-amplifier, and then measured using an HP 4194A Impedance/Gain-Phase Analyzer. The ac current is supplied by an ac voltage from the HP 4194A Analyzer through a non-inductive load resistor $R_L = 1$ kΩ, and the condition $R_L \gg Z_s$ (Z_s being the sample impedance) is satisfied for the entire experimental frequency range, to ensure a constant amplitude for the applied current. All measurements are performed in the linear response region, so that there is no variation of the impedance signal as a function of the applied

current. More details of the experimental set up are given in Refs. [30,31].

To deconvolve the sample impedance Z_s from the measured signal Z_{meas} over a broad frequency range, careful calibrations must be made in order to remove the background distortion. The measured impedance Z_{meas} may be expressed in terms of a general form:

$$Z_{meas} = (Z_s + Z_{back})G(f)e^{i\theta(f)},$$

where $G(f)$ is the amplitude of the total gain, and $\theta(f)$ is the phase shift due to uncompensated cable length and phase distortion of the pre-amplifier, which is only dependent on the experimental setup rather than the sample, and Z_{back} is the complex background impedance. For the frequency range of our experiment, it is reasonable to assume that the sample impedance at $T \gg T_c$ is completely resistive, and that $Z_s \approx R_s \gg Z_{back}$, where R_s is the normal state resistance of the sample. Hence,

$$Z_{meas}(T \gg T_c) \approx R_s G(f)e^{\theta(f)}.$$

Knowing R_s from the dc transport measurements, both $G(f)$ and $\theta(f)$ can be determined by measuring the phase and amplitude of $Z_{meas}(T \gg T_c)$ [30]. We note that both $G(f)$ and $\theta(f)$ are independent of either the temperature or the sample, because the total gain $G(f)$ is primarily determined by the gain of the pre-amplifier as well as contributions from the end-to-end losses of the measurement system and impedance mismatch, and the phase $\theta(f)$ is also associated with the phase distortion of the experimental setup, as mentioned earlier.

Similarly, it is reasonable to assume that Z_{back} is independent of the temperature of the sample, because Z_{back} includes parasitic capacitance and inductance of the measurement system, which is not a sensitive function of the sample temperature. Therefore, by measuring a short in the place of a superconductor, we have $Z_{meas} \approx Z_{back}G(f)e^{i\theta(f)}$, and Z_{back} can be determined by using the calibrated $G(f)$ and $\theta(f)$. Thus, the longitudinal impedance, Z_s, and therefore the longitudinal complex conductivity $\sigma_{xx}(f)$ for frequencies from 100 to 10^7 Hz can be obtained from the above calibration procedure.

In the case of Hall conductivity measurements, the calibration for the Hall impedance is more staightforward than that for the ac longitudinal impedance, because most parasitic background signals are invariant under the reversal of the applied magnetic field. Assuming that the net Hall signal is $Z_{s,Hall}$, we may express the measured signal $Z_{meas,Hall}$ as follows:

$$Z_{meas,Hall} = (Z_{s,Hall} + Z_{back,Hall})G(f)e^{i\theta(f)},$$

where $Z_{back,Hall}$ is a complex background signal, which includes not only the parasitic impedances of the experimental set up, but also contributions from the longitudinal impedance due to possible misalignment of the electrical contacts. In general, $Z_{back,Hall}$ is invariant under the reveral of the applied magnetic field. Therefore, we may remove $Z_{back,Hall}$ by performing measurements under both $+H$ and $-H$, and obtain

$$Z_{meas,Hall,corr} \equiv [Z_{meas,Hall}(H) - Z_{meas,Hall}(-H)]/2 = Z_{s,Hall}G(f)e^{i\theta(f)}.$$

Knowing $G(f)$ and $\theta(f)$ from the calibration procedure for the longitudinal impedance, we obtain $Z_{s,Hall}$ as a function of T, H and f.

The above calibration procedure has been applied to measurements of an expitaxial $YBa_2Cu_3O_{7-\delta}$ thin film on $LaAlO_3$ (100) substrate. The standard procedure for preparing these $YBa_2Cu_3O_{7-\delta}$ epitaxial films is as follows: The films were fabricated using the pulsed laser deposition technique under 400 mTorr oxygen vapor pressure, with the substrate temperature during the deposition at 800°C. After deposition, samples were slow-cooled to room temperature in 500 Torr of oxygen. More information about the fabrication and characterization of these $YBa_2Cu_3O_{7-\delta}$ epitaxial films are detailed in Ref. [34]. In this work, the frequency range of the ac longitudinal and Hall impedance measurements was from 10^2 Hz to 7×10^6 Hz, the temperature range from $T = 80.0$ K to 100.0 K, and all measurements were performed at constant magnetic fields of $H = 0$, 1, 2, 3, 4, and 5 Tesla, oriented along the sample c-axis. The applied current was always perpendicular to the magnetic field. The superconducting transition temperature T_c determined from dc resistive measurement for these films was typically between 87.5 to 89.5 K. In the following, results on a representative epitaxial film are shown, with $T_c \approx 88.2$ K, a transition width $\Delta T_c \approx 0.6$ K, and a normal state resistivity $\rho_{xx} \approx 100$ $\mu\Omega$ cm just above T_c.

IV. Results and Analysis

Following the calibration procedures outlined above, we obtain the frequency dependence of the real and imaginary parts of the longitudinal and Hall resistivity at various temperatures and fields, as exemplified in Figs.1(a)–(b) for ρ'_{xx} and ρ''_{xx} and in Figs.2(a)–(b) for ρ'_{xy} and ρ''_{xy}, with an applied field $H = 2$ T. Using Eq.(8), the corresponding Hall conductivity can be converted from the measured ρ_{xx} and ρ_{xy}, and the representative results for $H = 2$ T are shown in Figs.3(a)–(b) for σ'_{xy} and σ''_{xy} versus f at various T. We note that the same frequency dependence is observed for all isotherms taken at other magnetic fields, as illustrated in Figs.4(a)–(b) for σ'_{xy}-vs.-f and σ''_{xy}-vs.-f data taken at $T = 86.0$ K and $H = 1$, 2, 3, 4, and 5 T. For the magnetic field dependence of σ'_{xy} and σ''_{xy}, a representative set of data for $f = 1$ MHz is shown in Figs.5(a)–(b).

To verify the correctness of our experimental results, we first examine the zero-field longitudinal resistivity data, and find that the temperature and frequency dependence of the complex resistivity is consistent with the Drude model, with $\rho'_{xx} \sim$ constant and $\rho''_{xx} \propto \omega$, as discussed in Section II-B. Furthermore, in the low frequency limit and under finite magnetic fields, the real part of the complex Hall resistivity, ρ'_{xy}, recovers results obtained from the dc measurements, showing anomalous sign reversal for both $\rho'_{xy} - vs. - T$ and ρ'_{xy}-vs.-B in the vortex state [12]. In addition, the frequency dependence of both the real and imaginary parts of the complex Hall conductivity follows the prediction of Eq.(7), with $|\sigma'_{xy}| \sim$ constant and $|\sigma''_{xy}| \propto \omega$.

Regarding the magnetic field dependence of σ_{xy} in the vortex state, we note that previous coherence time-domain spectroscopy studies of the vortex-state complex Hall conductivity at high frequencies (from 100 GHz to 800 GHz) have attributed the vortex-state Hall effect solely to the non-localized quasiparticle contribution [7]. As stated in Section II, this assumption would imply $(\sigma'_{xy}/\sigma_0) \approx \omega_c\tau \propto B$ and $(\sigma''_{xy}/\sigma_0) \approx 2\omega_c\omega\tau^2 \propto B$ for $\omega \gg \omega_c$, which is different from the observed magnetic field dependence of our σ_{xy} data for frequencies up to 10^7 Hz. On the other hand, if we take into account the vortex contribution in the Hall conductivity, in the sign reversal regime where $\omega_c\tau \ll 1$, $\omega_0\tau \ll 1$, and

$g \to 0$, we find

$$\begin{aligned}
\sigma'_{xy} &\approx \frac{ne}{B}\left[g(\omega_0\tau)^2 - \left(\frac{\delta n}{n}\right) + (1-g)(\omega_c\tau)^2\right] \\
&\approx \frac{ne}{B}\left[-\left(\frac{\delta n}{n}\right) + \left(\frac{eB\tau}{m^*}\right)^2\right] \equiv \left[-\frac{c_1}{B} + c_2 B\right], \\
\sigma''_{xy} &\approx (-2\omega\tau)\frac{ne}{B}\left[g\omega_0^2\tau^2 - \frac{(\delta n/n)}{\omega_c^2\tau\tau_\infty} + (1-g)\omega_c^2\tau^2\right] \\
&\approx (-2\omega\tau)\frac{ne}{B}\left\{-\left(\frac{\delta n}{n}\right)\left[\frac{(m^*)^2}{e^2B^2\tau\tau_\infty}\right] + \left(\frac{eB\tau}{m^*}\right)^2\right\} \\
&\equiv \left[\frac{d_1}{B^3} - d_2 B\right], \qquad (9)
\end{aligned}$$

where c_1, c_2, d_1 and d_2 are positive coefficients. Fitting the σ'_{xy}-vs.-B data for $(T/T_c) \approx 0.97$ in Fig.5(a) using Eq.(9), we obtain $c_2 \equiv ne^3\tau^2/(m^*)^2 = 1140 \pm 50\ \Omega^{-1}\mathrm{m}^{-1}\mathrm{T}^{-1}$, where m^* is the effective mass of the carriers. Using $\tau \sim 0.3 \times 10^{-13}$ s determined from the dc Hall conductivity measurements at $(T/T_c) \sim 0.97$ [12], we have the total carrier density $n \approx 2.5 \times 10^{20}(m^*/m_e)^2\ \mathrm{cm}^{-3}$. For $(m^*/m_e) \approx 4$ in the case of $YBa_2Cu_3O_{7-\delta}$ [13,22], we obtain $n \approx 4 \times 10^{21}\mathrm{cm}^{-3}$, which is a reasonable value for $YBa_2Cu_3O_7$. Furthermore, using the fitting parameter $c_1 \equiv (ne)(\delta n/n) = (1.4 \pm 0.1) \times 10^4\ \Omega^{-1}\mathrm{m}^{-1}\mathrm{T}$ for $(T/T_c) \sim 0.97$, we obtain $(\delta n/n) \sim 2 \times 10^{-5}$, which is of the same order of magnitude as the theoretical estimate of $(\delta n/n) \sim [\Delta_0(T)/E_F]^2$ [10], assuming $\Delta_0(T) = \Delta_0[1-(T/T_c)]^{1/2}$ [10,12], and $\Delta_0 \approx 19meV$ is the average superconducting gap of $YBa_2Cu_3O_{7-\delta}$ [35]. On the other hand, we note that similar fitting to the imaginary part of the Hall conductivity σ''_{xy} yields $|\sigma''_{xy}/\sigma'_{xy}| \sim (d_2/c_2) \sim 10^{-2}$, which is much larger than the theoretical prediction of $|\sigma''_{xy}/\sigma'_{xy}| \sim (2\omega\tau) \sim 10^{-6}$ for $f = 1$ MHz. This discrepancy may be due to the incorrect assumption of s-wave pairing symmetry in $YBa_2Cu_3O_{7-\delta}$, as discussed in the next section.

V. Discussion

We have shown in the previous section that the magnetic field dependence of our experimental data manifest both contributions from quasiparticles and vortices to the vortex-state Hall conductivity. In addition, the temperature and frequency dependence of the complex

Hall conductivity is found to be consistent with our generalized FGLV model. Quantitatively, we also note that the real part of the Hall conductivity, σ'_{xy}, is in good agreement with the dc Hall conductivity data at radio frequencies. On the other hand, the magnitude of the imaginary part of the Hall conductivity, σ''_{xy}, is found to be much larger than the prediction based on the simple approximation outlined above.

One plausible explanation for this discrepancy is that the FGLV model does not consider the relevance of d-wave pairing symmetry in hole-type high-temperature superconductors, and therefore cannot account for the electronic structures correctly in the σ^v_{xy} term. More specifically, it has been shown that for an infinite size sample, a pure $d_{x^2-y^2}$ pairing symmetry prohibits any true bound state for quasiparticles around a vortex [16], in sharp contrast to a large number of bound states in conventional s-wave superconductors [14,15,19]. Consequently, the semi-classical approximation in Eq.(4b), which assumes an isotropic gap $\Delta_0 \ll E_F$ [19], must be modified in the case of pure d-wave pairing symmetry. On the other hand, we note that a small out-of-phase mixed symmetry (such as d_{xy} or s) relative to the predominant $d_{x^2-y^2}$ symmetry is expected in $YBa_2Cu_3O_{7-\delta}$ due to its orthorhombicity [35], and the existence of either $(d_{x^2-y^2} + id_{xy})$ [16,36,37] or $(d_{x^2-y^2} + is)$ mixed symmetries has several important implications on the Hall conductivity. First, a finite number of bound states with large energy spacing becomes available if mixed symmetries exist [16,38,39], so that the semi-classical approximation undertaken in Eq.(4b) remains valid. Second, the superconducting energy gap Δ_0 has to be replaced by Δ_k, where the wave-vector dependent energy gap is given by $\Delta_k = \Delta_d \cos 2\theta_k + i\Delta_s$ for the $(d_{x^2-y^2} + is)$ pairing symmetry, with $\Delta_d \gg \Delta_s$, and θ_k is the angle of the wave-vector relative to the antinode of the $d_{x^2-y^2}$ gap. Third, the characteristic frequency ω_0 in Eq.(4b) must be rewritten to incorporate the complex gap function and its spatial variation. Assuming that Eq.(4b) may be modified by replacing ω_0 with a complex characteristic frequency that reflects the mixed pairing symmetries in $YBa_2Cu_3O_{7-\delta}$, an increase in $|\sigma''_{xy}|$ may be expected without incurring noticeable decrease in $|\sigma'_{xy}|$ if $|\sigma''_{xy}| \ll |\sigma'_{xy}|$. However, rigorous theory which explicitly includes the correct pairing symmetry in the vortex-state

Hall conduction will be needed to quantitatively account for our experimental observation.

Another interesting aspect is the correlation of the sign of σ_{xy} with the doping level and the pairing symmetry. As stated in the introduction, the occurrence of sign reversal in the vortex-state σ_{xy} is associated with the condition $\delta n(\equiv n_0 - n_\infty) > 0$ in type-II superconductors, and δn is related to the quasiparticle bound states within the vortex core. We have noted that the orthorhombic structure of $YBa_2Cu_3O_{7-\delta}$ is likely to yield mixed pairing symmetries, and therefore can allow quasiparticle bound states in the vortex core, as manifested by the scanning tunneling spectroscopy studies of the vortex core states in $YBa_2Cu_3O_{7-\delta}$ [38]. Thus, the magnitude of δn is expected to be finite, and sign reversal may occur in the vortex-state σ_{xy} if $\delta n > 0$, according to Eq.(1). Similarly, the electron-type superconducting cuprate $Nd_{1.85}Ce_{0.15}CuO_4$ is known to be of the s-wave pairing symmetry [40]. Hence, quasiparticle bound states exist within the vortex core, and δn is finite. The observed sign reversal in the vortex-state Hall conductivity [9] therefore suggests that $\delta n > 0$. On the other hand, for pure tetragonal lattice structure of other hole-type superconducting cuprates, it is known that the pairing symmetry is $d_{x^2-y^2}$, and that no quasiparticle bound states may exist within the vortex core, as manifested in the scanning tunneling spectroscopy data by Renner et al. [41] on both the underdoped and overdoped $Bi_2Sr_2CaCu_2O_{8+\delta}$. If one naively associates the absence of quasiparticle bound states with the absence of vortex charging effect, *i.e.*, $\delta n = 0$, one would conclude that sign reversal could not occur in the vortex state Hall conductivity for either underdoped or overdoped $Bi_2Sr_2CaCu_2O_{8+\delta}$. However, the observation of sign reversal in the underdoped $Bi_2Sr_2CaCu_2O_{8+\delta}$ [13] suggests that the vortex charging effect is not trivially associated with the existence of quasiparticle bound states in the vortex core. More experimental and theoretical work is clearly needed to consistently correlate the doping level and pairing symmetry with the vortex charging effect.

Finally, we compare our *rf* results with the higher frequency Hall conductivity data reported previously [7]. We note that previous high frequency measurements were performed in one magnetic field, 6 T, and were analyzed in terms of a simple two-fluid model without

including the vortex contribution. As detailed in previous sections of this article, the vortex contribution can be best manifested by studying the magnetic field dependence of the Hall conductivity, particularly in the low-field limit. That is, $|\sigma_{xy}^v| \propto B^{-1}$ while $\sigma_{xy}^q \propto B$, so that the magnitude of σ_{xy}^v diverges in the low field limit [2] and has an opposite sign to σ_{xy}^q in the vortex state. Hence, the vortex contribution to σ_{xy} cannot be manifested by simply considering the temperature and frequency dependence of σ_{xy}. For the sake of completeness, we examine in the following whether our generalized FGLV model in Eq.(4b) may be consistent with the temperature and frequency dependence of the high-frequency data reported in Ref.[7]. Using the parameters given in Ref. [7], where τ varies from $\sim 10^{-13}s$ near T_c to $\sim 10^{-12}s$ at $T \ll T_c$, and $\omega_c = (40\ \text{GHz})$, we find $(\omega_c\tau)^2 <\sim (\omega_0\tau)^2 < 1$ for the frequency range of 100 GHz to 800 GHz, and $(\omega\tau) \sim 1$, varying from greater to smaller than 1 with increasing temperature. We may further neglect the term associated with $(\delta n/n)$ in Eq.(4b) at high frequencies, because it is insignificant relative to other terms except near T_c. Hence, Eq.(4b) is reduced into the following simple expression:

$$\sigma_{xy} \approx \frac{ne}{B}\left[\frac{g(\omega_0\tau)^2}{(1-\omega^2\tau^2)+\omega_0^2\tau^2-i2\omega\tau} + \frac{(1-g)(\omega_c\tau)^2}{(1-\omega^2\tau^2)+\omega_c^2\tau^2-i2\omega\tau}\right]. \qquad (10)$$

Thus, for a given frequency, the magnitude of both σ_{xy}' and σ_{xy}'' reaches a maximum if $\omega\tau \sim 1$. Since $\tau(T)$ decreases with increasing temperature and $\tau(T_{pk}) \sim \omega^{-1}$, the temperature T_{pk} at which $|\sigma_{xy}|$ reaches maximum is expected to *increase* with increasing frequency according to Eq.(10). Furthermore, Eq.(10) predicts that the magnitude of σ_{xy}'' becomes comparable to that of σ_{xy}' under the experimental conditions given in Ref. [7], consistent with the experimental data [7]. We therefore conclude that the complex vortex-state Hall conductivity given in Eq.(4b) contains most of the essential components, although full account for the quantitative details still awaits complete theoretical studies.

VI. Summary

In summary, we have investigated the complex Hall conductivity of $YBa_2Cu_3O_7$ epitaxial films at frequencies from 100 Hz to 7 MHz using a direct transport measurem

technique. An expression for the complex Hall conductivity in the flux-flow limit has been derived by generalizing the FGLV model for dc vortex-state Hall conductivity. We find that the *qualitative* behavior of the complex Hall conductivity data, including the dependence on temperature, frequency and magnetic field, can be described consistently with this generalized model. Furthermore, *quantitatively* the real part of the complex Hall conductivity recovers the dc Hall conductivity in the low frequency limit, and the carrier density n and the magnitude of the vortex charging effect ($\delta n/n$), derived from fitting σ'_{xy} data with our model, are found to be consistent with the known properties of $YBa_2Cu_3O_7$. In addition, in the high-frequency limit, our phenomenological model can also account for the temperature and frequency dependence of the coherent time-domain spectroscopy data taken at 100 GHz to 800 GHz. On the other hand, the magnitude of the imaginary part of the Hall conductivity (σ''_{xy}) at *rf* frequencies appears to be significantly larger than the prediction of our model. This discrepancy may be attributed to the unconventional electronic structures within the vortex core of cuprate superconductors with *d*-wave or mixed pairing symmetries. Further theoretical investigation which explicitly incorporates the correct pairing symmetry will be necessary to fully account for all aspects of the vortex-state Hall conductivity.

Acknowledgement

This work is jointly supported by NSF Grant #DMR-9705171, and the National Aeronautics and Space Administration, Office of Space Science (NASA/OSS). Part of the research was performed by the Center for Space Microelectronics Technology, the Jet Propulsion Laboratory, California Institute of Technology, and was sponsored by NASA/OSS.

Bibliography

[1] Y. Iye, S. Nakamura, and T. Tamegai, Physica C **159**, 616 (1989).

[2] A. T. Dorsey, Phys. Rev. B **46**, 8376 (1992); S. Ullah and A. T. Dorsey, Phys. Rev. B **44**, 262 (1991).

[3] S. J. Hagen, A. W. Smith, M. Rajeswari, J. L. Peng, Z. Y. Li, R. L. Greene, S. N. Mao, X. X. Xi et al., Phys. Rev. B **47**, 1064 (1993).

[4] V. M. Vinokur, V. B. Geshkenbein, M. V. Feigel'man, and G. Blatter, Phys. Rev. Lett. **71** 1242 (1993).

[5] J. M. Harris, Y. F. Yan, O. K. C. Tsui, Y. Matsuda, and N. P. Ong, Phys. Rev. Lett. **73**, 1711 (1994); J. M. Harris, N. P. Ong and Y. F. Yan, Phys. Rev. Lett. **71**, 1455 (1993).

[6] V. B. Geshkenbein and A. I. Larkin, Phys. Rev. Lett. **73**, 609 (1994)

[7] S. Spielman, B. Parks, J. Orenstein, D. T. Nemeth, F. Ludwig, J. Clarke, P. Merchant, and D. J. Lew, Phys. Rev. Lett. **73**, 1537 (1994); B. Parks et al., Phys. Rev. Lett. **74**, 3265 (1995).

[8] A. V. Samoilov, A. Legris, F. Rullieralbenque, P. Lejay, S. Bouffard, Z. Givanov, and L. G. Johansson, Phys. Rev. Lett. **74**, 2351 (1995).

[9] T. W. Clinton, A. W. Smith, Q. Li, J. L. Peng, R. L. Greene, C. J. Lobb, M. Eddy, and C. C. Tsuei, Phys. Rev. B **52**, R7046 (1995).

[10] M. V. Feigel'man, V. B. Geshkenbein, A. I. Larkin, and V. M. Vinokur, Pis'ma Zh. Eksp. Teor. Fiz. **62**, 811 (1995), (Engl. Transl. JETP Lett. **62**, 835 (1995)).

[11] A. van Otterlo, M. V. Feigel'man, V. B. Geshkenbein, and G. Blatter, Phys. Rev. Lett. **75**, 3736 (1995).

[12] D. A. Beam, N.-C. Yeh, and F. Holtzberg, J. Phys.: Condens. Matter **10** 5955 (1998).

[13] T. Nagaoka, Y. Matsuda, H. Obara, A. Sawa, T. Terashima, I. Chong, M. Takano, and M. Suzuki, Phys. Rev. Lett. **80**, 3594 (1998).

[14] A. G. Aronov, S. Hikami, and A. I. Larkin, Phys. Rev. B **51**, 3880 (1995); A. G. Aronov and A. B. Rapoport, Mod. Phys. Lett. B **6**, 1083 (1992).

[15] H. Fukuyama, H. Ebisawa, and T. Tsuzuki, Prog. Theor. Phys. **46**, 1028 (1971).

[16] M. Franz and Z. Tesanovic, Phys. Rev. Lett. **80**, 4763 (1998).

[17] D. A. Bonn, P. Dosanjh, R. Liang, and W. N. Hardy, Phys. Rev. Lett. **68**, 2390 (1992); D. A. Bonn, R. X. Liang, T. M. Riseman, D. J. Baar, D. C. Morgan, K. Zhang, P. Dosanjh, T. L. Duty, A. Macfarlane et al., Phys. Rev. B **47** 11314 (1993).

[18] P. Drude, Annalen der Physik **1**, 566 and **3**, 369 (1900).

[19] C. Caroli, P. G. de Gennes, and J. Matricon, Phys. Lett. **9**, 307 (1964).

[20] G. Blatter, M. V. Feigel'man, V. B. Geshkenbein, A. I. Larkin, V. M. Vinokur, Rev. Mod. Phys. **66** 1125 (1994).

[21] D. C. Mattis and J. Bardeen, Phys. Rev. **111**, 412 (1958).

[22] N.-C. Yeh and C. C. Tsuei, Phys. Rev. B **39**, 9708 (1989).

[23] K. Krishana, J. M. Harris, and N. P. Ong, Phys. Rev. Lett. **75**, 3529 (1995).

[24] D. A. Bonn et al., Phys. Rev. Lett. **68**, 2390 (1992); Phys. Rev. B **47**, 11314 (1993).

[25] N.-C. Yeh, D. S. Reed, W. Jiang, U. Kriplani, D. A. Beam, M. Konczykowski, F. Holtzberg, and C. C. Tsuei, in *Advances in Superconductivity – VII*, Vol.1, pg. 455–461, Springer-Verlag, Tokyo (1995).

[26] W. Jiang, N.-C. Yeh, D. S. Reed, D. A. Beam, U. Kriplani, M. Konczykowski, and F. Holtzberg, Phys. Rev. Lett. **72**, 550 (1994).

[27] N.-C. Yeh, D. S. Reed, W. Jiang, U. Kriplani, C. C. Tsuei, C. C. Chi, and F. Holtzberg, Phys. Rev. Lett. **71**, 4043 (1993).

[28] D. S. Reed, N.-C. Yeh, W. Jiang, U. Kriplani, and F. Holtzberg, Phys. Rev. B **47**, 6150 (1993).

[29] N.-C. Yeh, W. Jiang, D. S. Reed, U. Kriplani, F. Holtzberg, C. C. Tsuei and C. C. Chi, Physica A **200**, 374 (1993).

[30] D. S. Reed, Ph.D. thesis, Department of Physics, California Institute of Technology, (1995).

[31] D. A. Beam, Ph.D. thesis, Department of Physics, California Institute of Technology, (1997).

[32] L. Onsager, Phys. Rev. **38**, 2265 (1931).

[33] L. J. van der Pauw, Philips Res. Reports **13**, 1 (1958); *ibid* **16**, 187 (1961).

[34] M. C. Foote et al., Physica C **201**, 176 (1992).

[35] J. Y. T. Wei, N.-C. Yeh, D. F. Garrigus, and M. Strasik, Phys. Rev. Lett. **81**, 2542 (1998).

[36] K. Krishana et al., Science **277**, 83 (1997).

[37] R. B. Laughline, Phys. Rev. Lett. **80**, 5188 (1998).

[38] I. Maggio-Aprile et al., Phys. Rev. Lett. **75**, 2754 (1995).

[39] K. Karrai et al., Phys. Rev. Lett. **69**, 355 (1992).

[40] S. M. Anlage et al., Phys. Rev. B**50**, 523 (1994); J. A. Mao et al., Physica C **235**, 2013 (1995).

[41] Ch. Renner et al., Phys. Rev. Lett. **80**, 3606 (1998); Phys. Rev. Lett. **80**, 149 (1998)

Fig.1 Frequency-dependent isotherms of the complex longitudinal resistivity of a representative $YBa_2Cu_3O_7$ epitaxial film for $H = 2$ Tesla and $\vec{H} \parallel \hat{c}$: **(a)** ρ'_{xx}-vs.-f; **(b)** ρ''_{xx}-vs.-f. We note that each isotherm constitutes 400 data points, and that the shaded data of the isotherm at 100 K in **(b)** indicates the region where validity of data is questionable due to signal overloading the pre-amplifier in the normal state [31].

Fig.2 Frequency-dependent isotherms of the complex Hall resistivity of a representative $YBa_2Cu_3O_7$ epitaxial film for $H = 2$ Tesla and $\vec{H} \parallel \hat{c}$: **(a)** ρ'_{xy}-vs.-f; **(b)** ρ''_{xy}-vs.-f.

Fig.3 Frequency-dependent isotherms of the complex Hall conductivity derived from the results shown in Figs.1 and 2: **(a)** σ'_{xy}-vs.-f; **(b)** σ''_{xy}-vs.-f. (Note: the 88 K and 89 K data are plotted as $-\sigma''_{xy}$.)

Fig.4 Frequency-dependent complex Hall conductivity at various constant magnetic fields and for $T = 86.0K$. **(a)** σ'_{xy}-vs.-f; **(b)** σ''_{xy}-vs.-f. (Note: 4 Tesla and 5 Tesla data are plotted as $-\sigma''_{xy}$.)

Fig.5 Magnetic field dependence of the complex Hall conductivity at $T = 86.0$ K and $f = 1$ MHz. **(a)** σ'_{xy}-vs.-B: The solid line represents a theoretical fit with $\sigma'_{xy} = -(c_1/B) + c_2 B$, where $c_1 = 1.43 \times 10^4 \mathrm{CT/m^3} = 1.43 \times 10^4\ \Omega^{-1}\mathrm{m}^{-1}\mathrm{T}$, and $c_2 = 1.14 \times 10^3\ \Omega^{-1}\mathrm{m}^{-1}\mathrm{T}^{-1}$. **(b)** σ''_{xy}-vs.-B: The solid line represents a theoretical fit with $\sigma''_{xy} = (d_1/B^3) - d_2 B$, where $d_1 = 4.09 \times 10^2\ \Omega^{-1}\mathrm{m}^{-1}\mathrm{T}^3$, and $d_2 = 2.49\ \Omega^{-1}\mathrm{m}^{-1}\mathrm{T}^{-1}$.

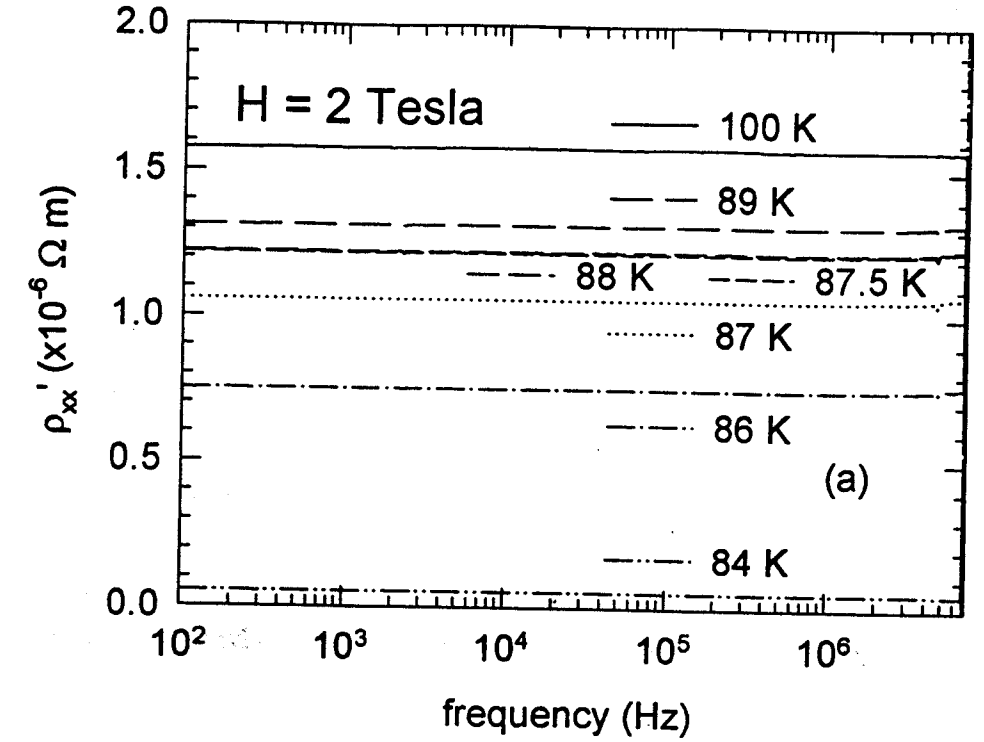
H = 2 Tesla
100 K
89 K
88 K
87.5 K
87 K
86 K
84 K
(a)
2.0
1.5
1.0
0.5
0.0
ρ_{xx}' (x10^{-6} Ω m)
10^2
10^3
10^4
10^5
10^6
frequency (Hz)

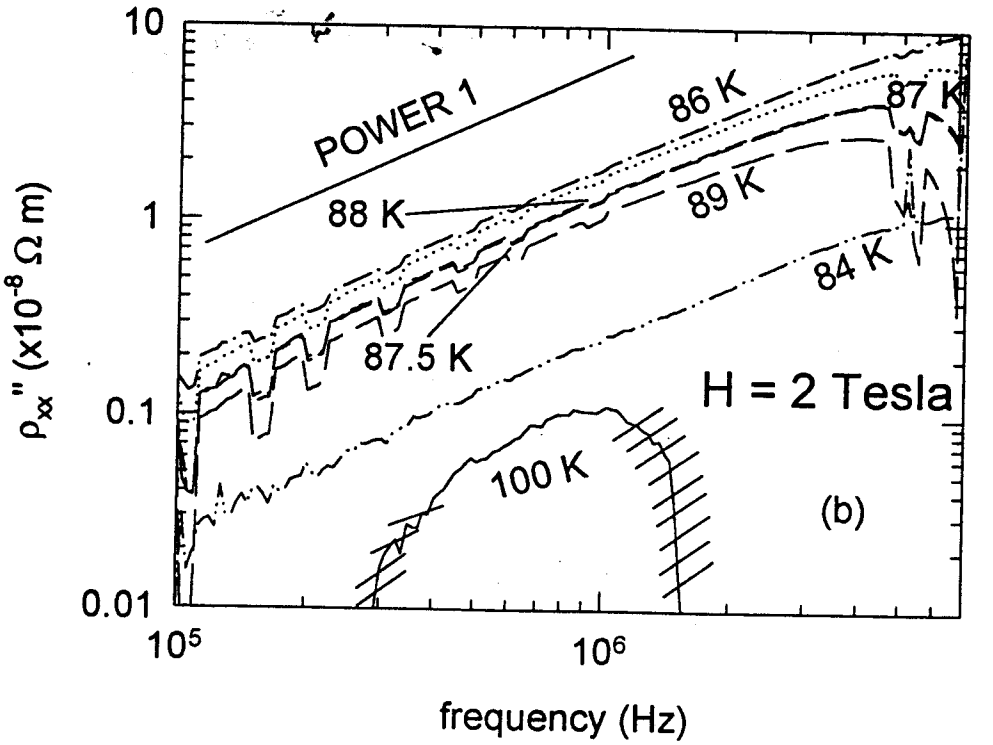
POWER 1
86 K
87 K
88 K
89 K
84 K
87.5 K
H = 2 Tesla
100 K
(b)
10
1
0.1
0.01
ρ_{xx}'' (x10^{-8} Ω m)
10^5
10^6
frequency (Hz)

Figure 1

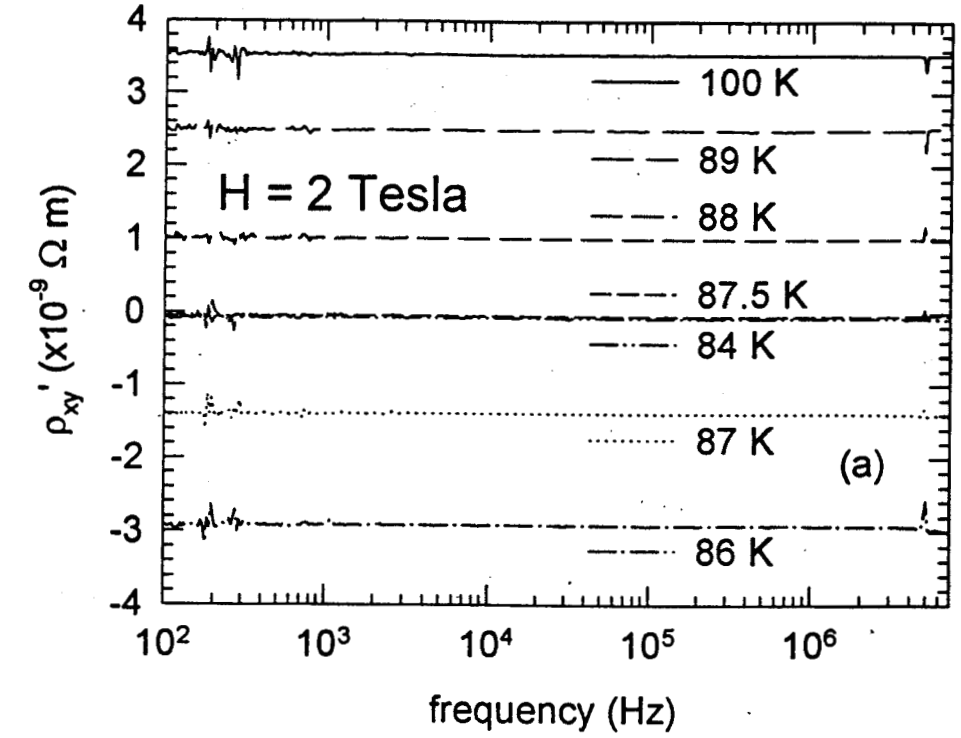
H = 2 Tesla
100 K
89 K
88 K
87.5 K
84 K
87 K
86 K
(a)
ρ_{xy}' (x10^{-9} Ω m)
frequency (Hz)

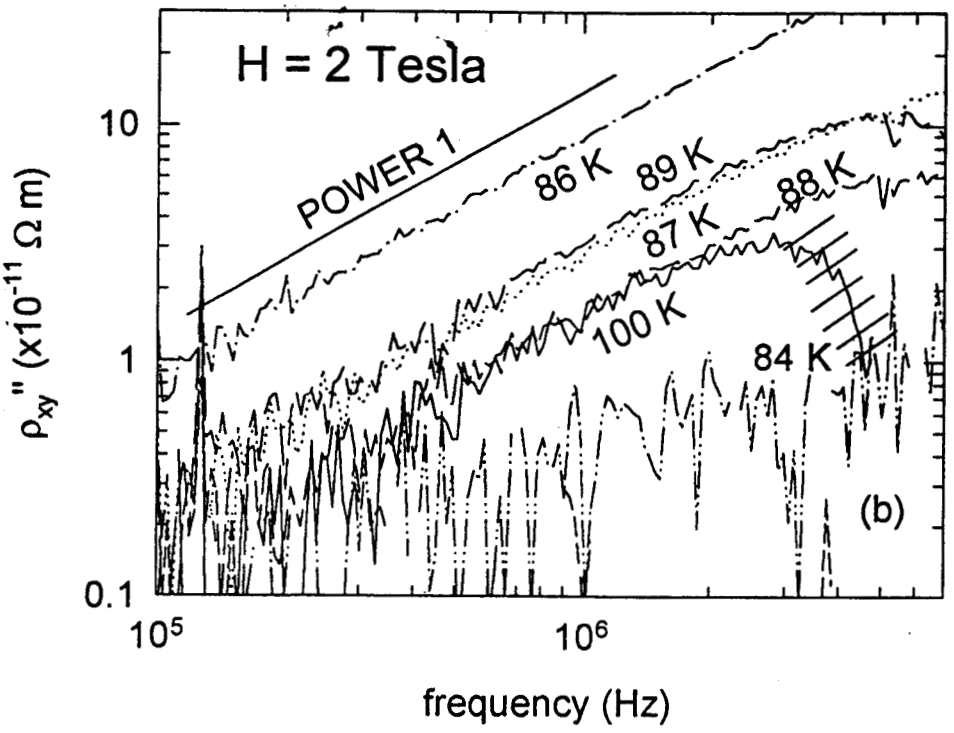
H = 2 Tesla
POWER 1
86 K
89 K
88 K
87 K
100 K
84 K
(b)
ρ_{xy}'' (x10^{-11} Ω m)
frequency (Hz)

Figure 2

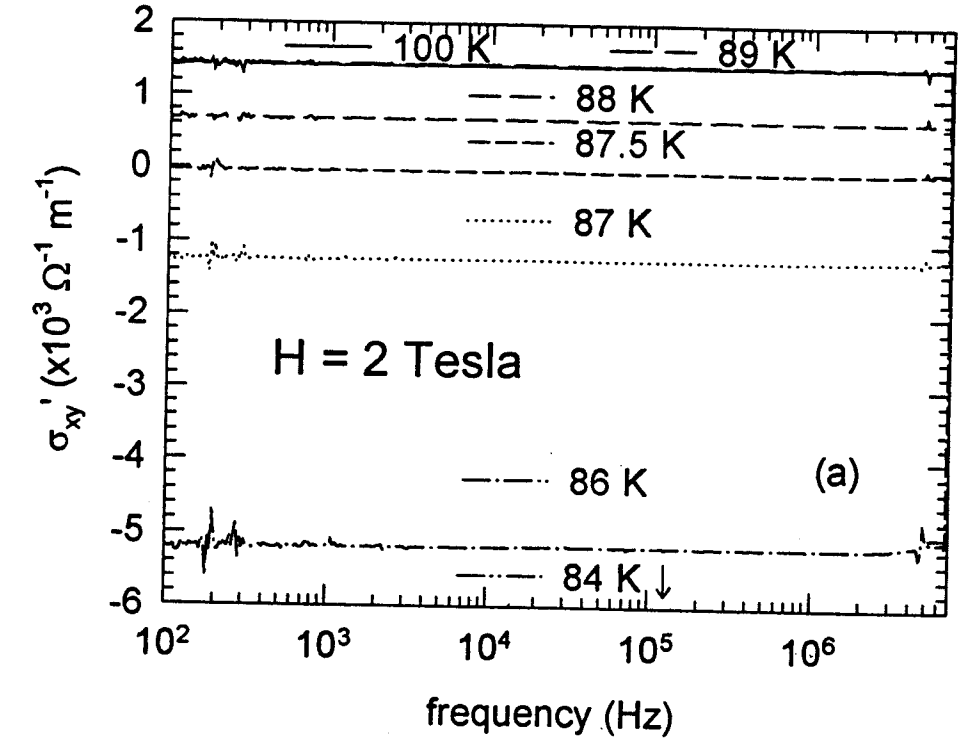
100 K
89 K
88 K
87.5 K
87 K
H = 2 Tesla
86 K
(a)
84 K
σ_{xy}' (x10^3 Ω^{-1} m^{-1})
frequency (Hz)

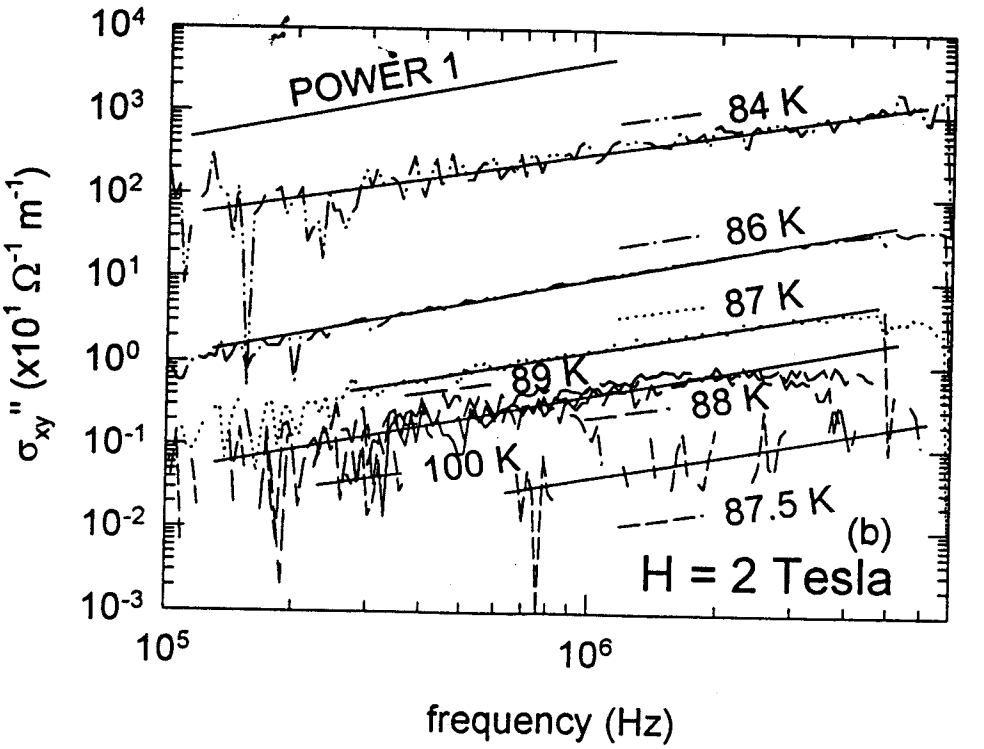
POWER 1
84 K
86 K
87 K
89 K
88 K
100 K
87.5 K
(b)
H = 2 Tesla
σ_{xy}'' (x10^1 Ω^{-1} m^{-1})
frequency (Hz)

Figure 3

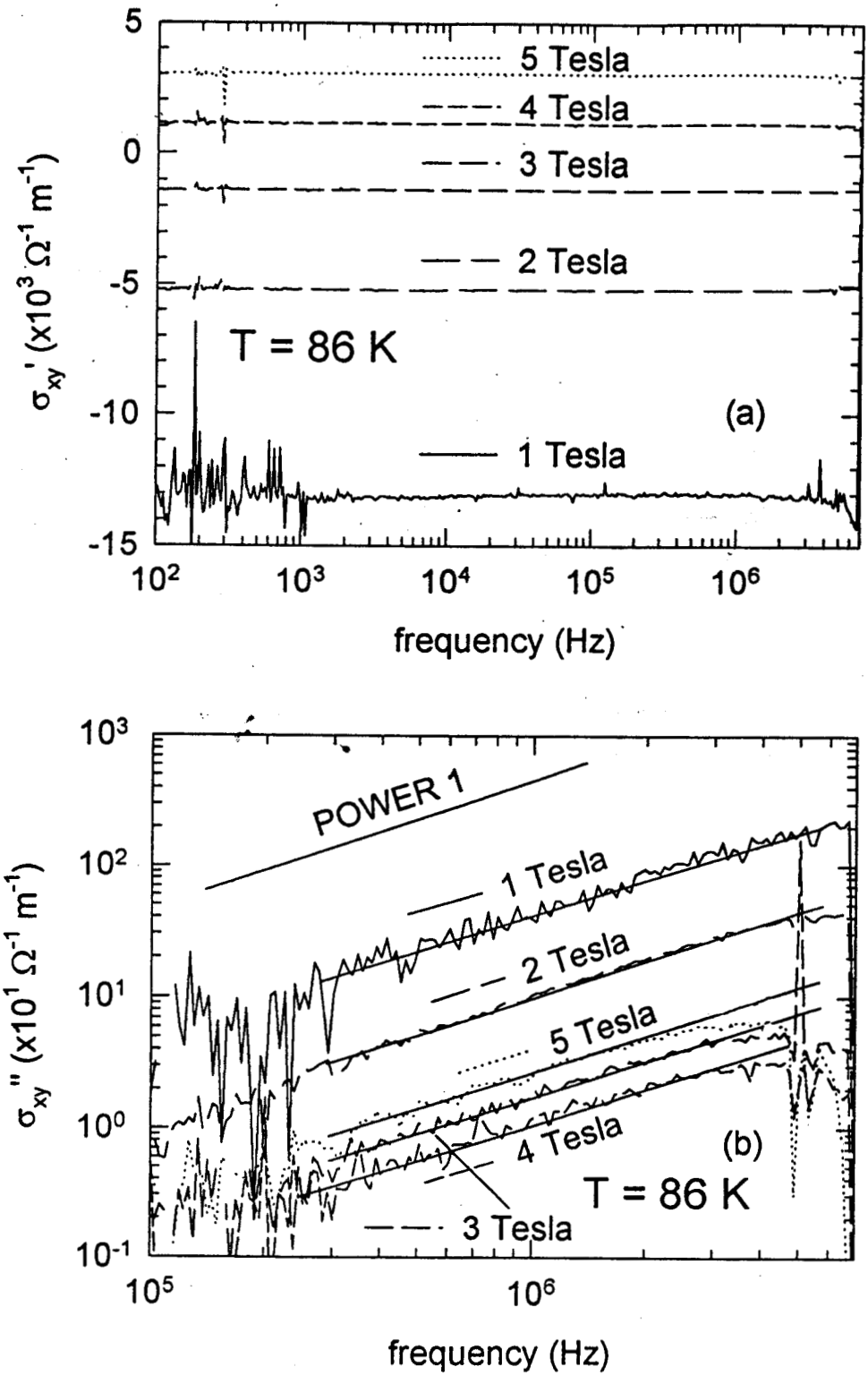
5
0
-5
-10
-15
σ_{xy}' (x10^3 Ω^{-1} m^{-1})
5 Tesla
4 Tesla
3 Tesla
2 Tesla
1 Tesla
T = 86 K
(a)
10^2
10^3
10^4
10^5
10^6
frequency (Hz)
10^3
10^2
10^1
10^0
10^{-1}
σ_{xy}'' (x10^1 Ω^{-1} m^{-1})
POWER 1
1 Tesla
2 Tesla
5 Tesla
4 Tesla
3 Tesla
(b)
T = 86 K
10^5
10^6
frequency (Hz)

Figure 4

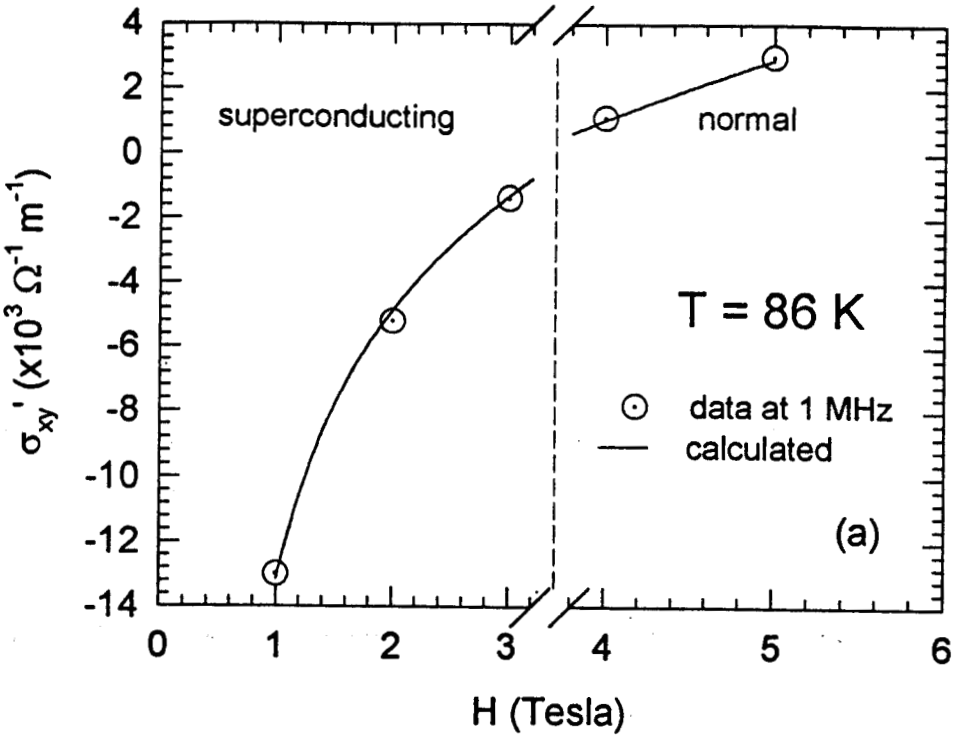
superconducting
normal
T = 86 K
data at 1 MHz
calculated
(a)
σ_{xy}' (x10^3 Ω^{-1} m^{-1})
H (Tesla)

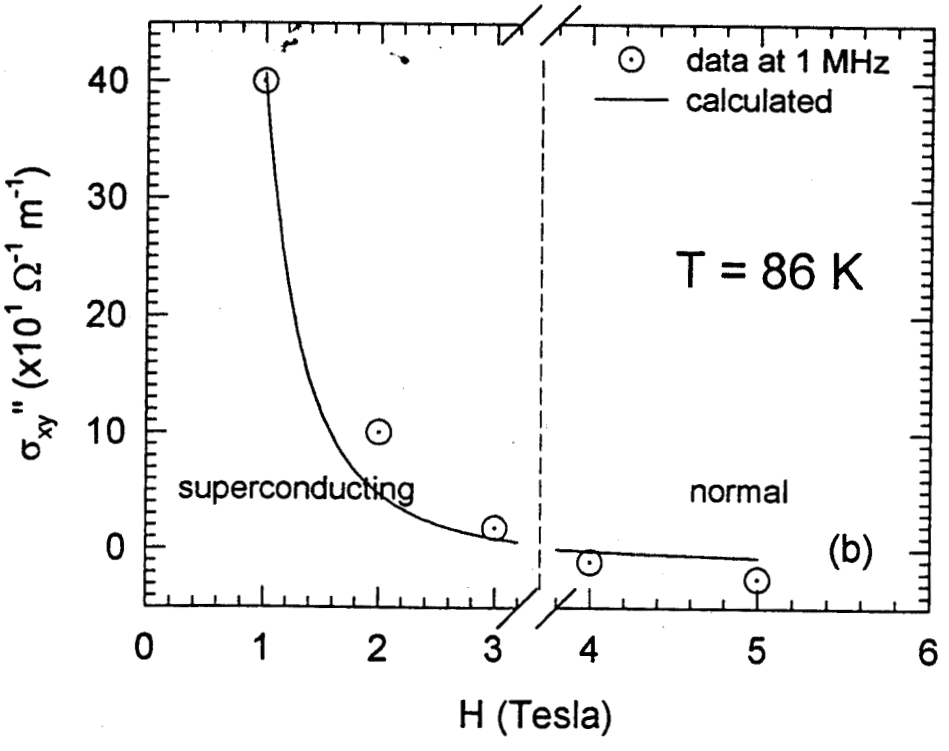
data at 1 MHz
calculated
T = 86 K
superconducting
normal
(b)
σ_{xy}'' (x10^1 Ω^{-1} m^{-1})
H (Tesla)

Figure 5